RESTRICTED

RM E50L20

NACA RM E50L20

NACA

RESEARCH MEMORANDUM

AVERAGE OUTSIDE-SURFACE HEAT-TRANSFER COEFFICIENTS AND VELOCITY DISTRIBUTIONS FOR HEATED AND COOLED IMPULSE TURBINE BLADES IN STATIC CASCADES

By James E. Hubbartt and Eugene F. Schum

Lewis Flight Propulsion Laboratory
Cleveland, Ohio

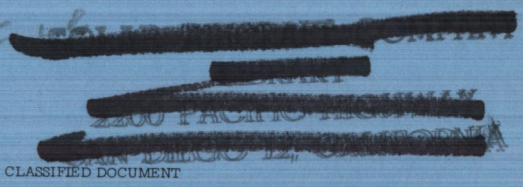

CLASSIFIED DOCUMENT

This document contains classified information affecting the National Defense of the United States within the meaning of the Espionage Act, USC 50:31 and 32. Its transmission or the revelation of its contents in any manner to an unauthorized person is prohibited by law.

Information so classified may be imparted only to persons in the military and naval services of the United States, appropriate civilian officers and employees of the Federal Government who have a legitimate interest therein, and to United States citizens of known loyalty and discretion who of necessity must be informed thereof.

NATIONAL ADVISORY COMMITTEE FOR AERONAUTICS

WASHINGTON
March 9, 1951

RESTRICTED

NATIONAL ADVISORY COMMITTEE FOR AERONAUTICS

RESEARCH MEMORANDUM

AVERAGE OUTSIDE-SURFACE HEAT-TRANSFER COEFFICIENTS AND VELOCITY DISTRIBUTIONS FOR HEATED AND COOLED IMPULSE TURBINE BLADES IN STATIC CASCADES

By James E. Hubbartt and Eugene F. Schum

SUMMARY

A heat-transfer investigation was conducted on cooled as well as heated impulse-type turbine blades in a static cascade to determine the effect of direction of heat flow on convective heat-transfer coefficients. In addition to the heat-transfer data, velocity distributions around the blade were experimentally measured and compared with the velocities calculated from a theory derived herein. The experimental heat-transfer coefficients were compared with theoretically derived coefficients that were dependent on the experimental velocity distribution around the blade periphery. The investigations were conducted over a range of air temperature from 60° to 600° F. The Reynolds number ranged from 10,000 to 100,000 and the gas-to-blade temperature ratio ranged from 0.9 to 1.1.

It was found that:

(a) The heated- and cooled-blade heat-transfer coefficients could be correlated by use of a Nusselt, Prandtl, and Reynolds number relation when the Reynolds number was multiplied by the ratio of effective gas temperature to average blade temperature.

(b) The blade peripheral-velocity distributions calculated from theory were approximately 20 percent lower than experimentally measured velocities in the central portion of the blade.

(c) The theoretically predicted heat-transfer rates based on an experimental velocity distribution were within 1 and 4 percent of the experimental heated- and cooled-blade results, respectively, at a

Reynolds number of 75,000; but at a Reynolds number of 15,000, these differences were 10 and 23 percent, respectively.

(d) The 23-percent error in gas-to-blade heat-transfer coefficient could cause an error in the calculation of blade temperatures of the order of 50° F for a blade temperature of 1000° F, turbine-inlet temperature of 1600° F, and a coolant temperature of 500° F. This error is somewhat large. For many materials, a 50° F change in blade temperature at 1000° F appreciably affects blade life.

INTRODUCTION

Outside-surface heat-transfer coefficients for static cascades of turbine blades ranging from impulse to high-percent reaction blades have been experimentally obtained by several investigators (references 1 to 5). In most cases, the blades were heated instead of cooled and using the heated data for an application in a turbine where the blade is cooled may not be justified. It is shown in reference 6 that the heat-transfer coefficients obtained on a cooled turbine under actual operating conditions agreed well with results obtained with impulse blades of similar shape in static cascade investigations, in which one set of blades was heated and another set was cooled. It should be noted that the effects of heating or cooling, rotation, and separation cited in reference 6 may have influenced this comparison.

A theory for predicting the convective heat-transfer coefficients for turbine blades is presented in reference 7, in which the gas-to-blade temperature ratio was assumed to be approximately 1. Good agreement is shown in reference 7 between the theory and the results of experimental static cascade investigations. Application of this heat-transfer theory requires knowledge of the velocity distribution around the blade periphery. Because these velocities were not experimentally measured in the cascade investigations, velocity distributions were calculated by means of the stream-filament theory, as described in reference 8. Although good agreement between the velocity distribution as calculated by this stream-filament theory and the experimental results has been obtained for a limited number of reaction-type blades (reference 8), the theory is dependent upon assumptions that may not be applicable to all blade shapes. Assumptions that are more applicable to impulse-type blades have been incorporated into a modification of the stream-filament theory that is derived herein.

Little experimental heat-transfer data are available on cooled blades and no comparison is available between the experimental and theoretical heat-transfer correlations in which these correlations are based on an experimental velocity distribution. An experimental investigation was therefore conducted at the NACA Lewis laboratory with a cascade of impulse turbine blades to determine (1) heat-transfer coefficients with the heat flow from blade to gas and from gas to blade, and (2) blade peripheral-velocity distributions. The velocity distributions around the blade periphery were measured and then compared with those predicted by the aforementioned stream-filament theory as modified herein for assumptions more applicable to the particular blade shape investigated. Finally, an experimental velocity distribution was used with the heat-transfer theory of reference 7 to obtain a theoretical correlation. The theoretical correlation was then compared with the experimental heat-transfer data.

THEORY

Convective gas-to-blade heat-transfer coefficients for turbine blades can be correlated by the following equation:

$$\frac{Nu}{Pr^{1/3}} = C(Re)^m \tag{1}$$

(The symbols are defined in appendix A.) It is shown in reference 7 that the constants C and m can be evaluated by means of boundary-layer theory and the resulting equation applied to turbine blades if the velocity distribution around the blade is known. Both C and m are functions of the average Euler number Eu_{av} in the laminar boundary layer and the transition ratio ξ. Plots of these functions are given in reference 7. The point of transition from laminar to turbulent boundary layer is assumed to occur where the pressure gradient first becomes zero (reference 7). Even though the Euler number is evaluated only in the laminar boundary layer, the theoretical Nusselt number or the gas-to-blade heat-transfer coefficient is an average value for the entire blade surface, including the turbulent boundary-layer region.

Because the velocity distribution is required for the theoretical evaluation of the constants C and m in equation (1), a method of analytically determining the velocity distribution for cases where it has not been or cannot be experimentally measured is necessary. For several reaction-type turbine blades, the velocity distribution predicted by the stream-filament theory of reference 8 agrees well with experiments. Such comparisons with impulse-type blades have not been made. The theory of reference 8 assumes that the curvature K of the

flow lines along an orthogonal line (line normal to the flow lines and connecting adjacent blade surfaces) varies according to the equation

$$K = K_1 + \frac{K_2 - K_1}{D} f \tag{2}$$

For many impulse-type blades (especially the type investigated herein), a better assumption would be to let the radius of curvature r of the flow lines vary linearly with f. The curvatures of the flow lines are therefore given by

$$\frac{1}{K} = r_1 + \frac{r_2 - r_1}{D} f \tag{3}$$

The stream-filament theory of reference 8 has been revised using equation (3) in the continuity equation, rather than equation (2). The derivation and the resulting equations for computing the velocities are given in appendix B. In order to predict the velocity distribution for any particular cascade of blades, the theory corresponding to the more accurate assumption (either equation (2) or equation (3)) should be applied. From the velocity distribution and the specified conditions, the average heat-transfer coefficient can be computed by equation (1) in conjunction with the curves of reference 7.

APPARATUS

The general arrangement of the apparatus is shown in figure 1 with the blades prepared for root cooling by the circulation of cooling water through a 3/8-inch water passage drilled in a bronze dummy-wheel section. For the heated-blade investigations, the cooling-water leads were removed and a small electric furnace was so located below the test section that the root section of the cascade protruded down into the furnace. Clean dry air at a pressure of 50 inches of mercury absolute was supplied and passed successively through a 90-kilowatt heater, a flat-plate orifice, a throttling valve, a large surge tank, the inlet nozzle, the test section, a throttle valve, and into the exhaust system where a pressure of 10 inches of mercury absolute was maintained. With maximum air flow, the inlet-air temperature could be varied from 60° to approximately 600° F.

Photographs of the blades and blade housings of the test section are shown in figure 2. A cross-sectional view of the blades with pertinent dimensions and instrumentation location is shown in figure 3. The blades, which were of constant cross-sectional area along the length, were shrouded at the tip to form a gas-flow passage 1 inch in height.

The apparatus was insulated with $1\frac{1}{2}$ inches of asbestos to reduce heat losses. For the cooled-blade investigations, additional loose-asbestos insulation was applied at the test section by filling a large box enclosing the test section. This additional insulation covered the entire portion of the test section where measurements were made. For the heated-blade investigations, use of additional insulation around the test section was unnecessary because the air passing over the blade surfaces was maintained at approximately room temperature. This fact was verified by tests made with and without the added insulation. Additional insulation, however, was applied between the electric furnace and the test section with only the bronze dummy-wheel section exposed to the electric furnace.

A radiation probe inside one blade was used to measure the radial-temperature distribution down the blade center (reference 4). The position of the probe was measured with an accuracy of approximately ±0.001 inch. Three fixed thermocouples were installed along the mean camber line in each of two blades (fig. 3) to check the validity of assuming a one-dimensional (radial) temperature distribution. In addition, two adjacent blades were drilled for eight static-pressure measurements with the pressure taps located in the center of the common flow channel. Five of these taps were located on the suction surface and three on the pressure surface, as shown in figure 3. These pressure taps provided an experimental method of obtaining the velocity distribution.

Inlet total- and static-pressure measurements were made just upstream of the blades. The total pressure was measured by a calibrated probe and the static pressure was measured by a wall tap. The outlet static pressure was determined by a fixed static-pressure probe. The inlet and outlet total gas temperatures were measured in the 6-inch ducts upstream and downstream of the test section where the velocity head was negligible. The estimated accuracy of measured temperature differences for use in equation (4) or (5) for the calculation of the heat-transfer coefficient is $\pm 1^{\circ}$ F.

PROCEDURE

The heat-transfer investigation was conducted over a range of Reynolds number from 10,000 to 100,000, which was obtained by varying the air flow from 0.04 to 0.40 pound per second. Most current turbines operate close to or above the upper limit of this range. The range of Reynolds number was limited by the available services and small blade dimensions. The ratio of the blade temperature to the gas temperature was varied from 0.9 to 1.1. For each run, thermal

equilibrium was assumed when the air temperature remained within approximately $\pm 1^{\circ}$ F for 5 minutes. After equilibrium was established the data were obtained. Blade temperatures were measured for 16 different positions varying from root to tip. Pressure measurements were made in the blade channel to determine the experimental-blade peripheral-velocity distribution.

CALCULATION METHODS

Heat-Transfer Coefficient

If, for a turbine blade that is heated or cooled at one end, it is assumed that (a) the blade is of constant cross-sectional area and perimeter along its length, (b) the temperature gradients in any cross section normal to the blade length are negligible, (c) the heat-transfer coefficient is constant along the blade length, (d) radiation can be neglected, and (e) at some position along the blade length the heat flow becomes zero, the temperature distribution with a constant blade-metal thermal conductivity can be given by (appendix C)

$$\theta = \theta_n \frac{\cosh \varphi(Y - y)}{\cosh \varphi Y} \tag{4}$$

or for a first-order correction for a variable thermal conductivity by

$$\theta = \left(\frac{\theta_n}{\cosh \varphi Y} - \frac{\lambda \theta_n^2 \cosh 2\varphi Y}{3 \cosh^3 \varphi Y} \right) \cosh \varphi(Y - y) + \lambda \theta_n^2 \frac{\cosh 2\varphi(Y - y)}{3 \cosh^2 \varphi Y} \tag{5}$$

where

$$\varphi = \sqrt{\frac{lH}{k_B A}} \quad \text{and} \quad k = k_B(1 - \lambda\theta)$$

The blade investigated was designed with a constant cross-sectional area and perimeter along its length, and the investigation was made under such conditions that the aforementioned assumptions were valid. Equation (5) could therefore be used to compute the heat-transfer coefficients. If the effect of a variable thermal conductivity is small, the much simpler equation (4) could be used. For this reason, equations (4) and (5) were compared by assuming values of H, k (as a function of θ), θ_n, and Y typical of those for the experiments. The temperature distributions predicted in this manner are compared in figure 4. The simpler equation (4) has been used for computing the

heat-transfer coefficients because the difference in the coefficient calculated by both equations is less than 2 percent.

Application of equation (4) for determining the heat-transfer coefficients for the blades investigated is discussed in reference 4. Briefly, this application consists in first determining θ as the difference between the effective gas and blade temperatures by the equation

$$\theta = T_{g,e} - T_{B,y} = \left[T' - (1 - \alpha)\frac{V_o^2}{2gJc_p}\right] - T_{B,y} \tag{6}$$

where the total gas temperature T' is evaluated as the average of the inlet and exit total gas temperatures, the recovery factor α is determined from the calibration curve of reference 4, and the velocity V_o is calculated by the equation

$$V_o^2 = 2gJc_pT'_o\left[1 - \left(\frac{p_o}{p'_o}\right)^{\frac{\gamma-1}{\gamma}}\right] \tag{7}$$

Then the values of Φ and Y, which permit equation (4) to most closely approximate the values of θ for the different positions of the blade probe thermocouple, can be computed by the method of least squares (reference 4). From Φ the heat-transfer coefficient is calculated.

The specific definition of each of the parameters as used to represent the heat-transfer results is given in appendix A. The inlet Reynolds numbers Re_i were evaluated with velocities and pressures computed from conditions measured at the blade inlet. The average Reynolds numbers Re_{av} were evaluated with the integrated average of the experimental velocities and pressures around the blade periphery.

Velocity Distribution

The experimental velocities around the blade periphery were also computed by use of equation (7) where velocity, temperature, and pressure subscripts are applied to the local conditions. Because the total temperature and pressure could not be measured in the blade passage, the total pressure was assumed constant through the passage and the local total temperature was defined as the average of the inlet and exit total temperatures. This determination of total temperature should be valid because the total-temperature change across the blades was an average of 5° F. The average velocity around the blade periphery

as used in Re was obtained with a planimeter from a plot of the experimental velocities in the center portion and the velocities on the leading and trailing portions of the blade faired in using circulation checks. This method gives an average velocity not sensitive to errors introduced by fairing in the velocities on the leading and trailing edges. The average pressure for use in Re was then computed by

$$p_{av} = p'_i \left(1 - \frac{V_{av}^2}{2gJc_p T'_{av}}\right)^{\frac{\gamma}{\gamma-1}} \tag{8}$$

The theoretical velocities around the blade periphery, which were desired for comparison with the experimental velocities, were determined by the compressible-flow theory described in appendix B.

RESULTS AND DISCUSSION

Experimental Heat-Transfer Results

A comparison of the heated- and cooled-blade heat-transfer results is shown in figure 5(a) on the basis of the inlet Reynolds numbers. The gas properties and the density are evaluated at the average blade temperature and the characteristic dimension is the blade perimeter divided by π. Good correlation is obtained in reference 5 when the physical properties of the gases are evaluated at this temperature. With the exception of the cooled-blade data for Reynolds numbers over 60,000, the data of figure 5(a) are represented within an accuracy of 4 percent by the corresponding mean lines. At a Reynolds number of 60,000, a definite change occurred in the relation between the cooled-blade heat-transfer rate and the Reynolds number. A satisfactory explanation of this change is unavailable at this time. For the remaining figures and discussion, the cooled-blade data above this critical region on the Nusselt plot will be deleted. The deviation between the heated- and cooled-blade data on figure 5(a) varied from approximately 16 percent at the low Reynolds numbers to approximately 3 percent at a Reynolds number of 60,000. The heated-blade data presented in this investigation are within 5 percent of the line representing the data presented in reference 4 and are well within the experimental scatter of data given in this reference.

In reference 5, it is shown that for comparing different sets of experimental heat-transfer results, better agreement is obtained when the Reynolds number Re is evaluated by the average pressure and average velocity around the blade periphery, instead of when the more convenient inlet Reynolds number Re_i is used. A comparison of the

heated- and cooled-blade data on the basis of equation (1), in which the average Reynolds number is used, is shown in figure 5(b). The comparison between the heated- and cooled-blade results is approximately the same as in figure 5(a); figure 5(b), however, presents the more representative procedure for comparing these results with those from other turbine blades.

A correlation in which the heated- and cooled-blade data fall on a single line is shown on figure 6, which was obtained by introducing the ratio of the effective gas temperature to the average blade temperature as a product in the abscissa of figure 5(b). The maximum deviation from the mean curve is ±5 percent, which is considered a good correlation. Even though good agreement does exist for these data, the experimental variation in the gas-to-blade temperature ratio ranged from 0.9 to 1.1 and caution should be employed for extrapolation to temperature ratios beyond these values until additional data are obtained. It is pointed out in reference 7 that a variation of the gas properties in the boundary layer may affect the rate of heat transfer. Temperature ratio and physical properties of the fluid enter into the boundary-layer equations in a complicated manner and a more rigorous theory is needed for the calculation of gas-to-blade heat-transfer coefficients that will include the effect of temperature ratio.

Experimental and Theoretical Velocity Distributions

A dimensionless plot of the experimental velocities around the cooled blade is shown in figure 7. Typical velocity distributions were chosen for this plot with the inlet Mach number varying from 0.185 to 0.412. The rapid rise in the velocity on the suction surface occurs near the region where the air enters the channeled portion of the blade, and also where the blade profile has a transition from a straight line to an arc. Both of these factors would contribute to an increasing velocity. Although the blade is symmetrical, the velocities on the suction surface are not symmetrical about the blade axis (about $x/L = 0.5$) showing that separation may exist somewhere after the midpoint of the surface.

A comparison of the heated- and cooled-blade velocity distribution is shown in figure 8. For both the low and high Mach numbers, the velocity ratios V_x/V_i are apparently independent of the direction of heat flow. For this reason, the comparison between the heated- and cooled-blade heat-transfer data in figure 5(a) was approximately the same as that in figure 5(b).

A comparison between the velocities predicted by the theory in appendix B and those experimentally determined for a representative run is shown in figure 9. The calculated velocities were approximately 20 percent lower than the experimental velocites in the central portion of the blade. Additional experimental data apparently are required from other impulse-blade cascades of different blade design before any definite conclusions can be reached concerning the calculation of the peripheral-velocity distributions.

Predicted Heat-Transfer Results

The heated- and cooled-blade results presented in figure 5(b) are compared in figure 10 with a theoretical correlation obtained by the method previously described (reference 7). The experimentally determined blade peripheral velocities were used in obtaining a theoretical heat-transfer correlation because it was believed that the experimental velocities were more accurate than the calculated velocities. Only one theoretical curve is obtained because the theory does not include a heating or cooling effect on heat transfer. At a high value of Reynolds number (75,000), the theoretical heat-transfer correlation agreed within 1 and 4 percent of the curves representing the heated- and cooled-blade data, respectively. At low Reynolds number (15,000), this agreement was approximately 10 and 23 percent for the heated and cooled blade, respectively. Because of the disagreement between the theoretical and experimental results at the low values of Reynolds number encountered in this investigation, it appears that additional refinements may be needed in the theory. Reynolds numbers encountered in current turbojet operations are usually above 100,000. For a small water-cooled turbine (reference 6) with a Reynolds number range of 30,000 to 100,000, excellent agreement was obtained between the experimental heat-transfer results and a theoretical correlation based on a calculated velocity distribution. Such close agreement was probably due to compensating errors, because the theoretical correlation did not consider effects of rotation, cooling, or heating of the blades and possible separation.

The calculated blade temperature is dependent upon the gas-to-blade heat-transfer coefficient. For example, with use of an assumed turbine-inlet gas temperature of 1600° F and a coolant temperature of 500° F, an error in the gas-to-blade heat-transfer coefficient of 23 percent (largest found in this investigation) could cause an error in calculated blade temperatures of the order of 50° F for a blade temperature of 1000° F. Methods described in reference 9 were used to determine this error. For many materials, a 50° F change in blade temperature at 1000° F appreciably affects the blade life; consequently, an error of 23 percent in the determination of the heat-transfer coefficient is somewhat large.

SUMMARY OF RESULTS

A heat-transfer investigation was conducted on cooled and heated impulse-type turbine blades in a static cascade to determine the effect of direction of heat flow on convective heat-transfer coefficients. Velocity distributions around the blade periphery were experimentally measured and were compared with velocities calculated from a theory derived herein. The experimental velocity distribution was then used to obtain a theoretical heat-transfer correlation.

For a range of inlet Reynolds number of 10,000 to 100,000 and a range of blade-to-gas temperature ratio of 0.9 to 1.1, the following results were obtained:

1. The heated- and cooled-blade heat-transfer data could not be represented by a common equation relating Nusselt, Prandtl, and average Reynolds numbers.

2. The experimental data were correlated by introducing the ratio of the effective gas temperature to the average blade temperature as a multiplier of the average Reynolds number in the Nusselt, Reynolds, Prandtl relation. Caution should be employed in the use of this correlation for ratios of the effective gas temperature to average blade temperature larger than those covered in this investigation.

3. The calculated velocities in the central portion of the blade were approximately 20 percent lower than the experimental velocities.

4. At high values of Reynolds number (75,000), the theoretical heat-transfer correlation based on an experimental velocity distribution over the blade periphery agreed within 1 and 4 percent, respectively, with the curve representing the heated- and cooled-blade data. At lower values of Reynolds number (15,000), this agreement was 10 and 23 percent, respectively.

5. For an assumed turbine-inlet gas temperature of 1600° F and a coolant temperature of 500° F, an error in the gas-to-blade heat-transfer coefficient of 23 percent (largest found in this investigation) could cause an error in calculated blade temperatures of the order of 50° F for a blade temperature of 1000° F.

Lewis Flight Propulsion Laboratory,
National Advisory Committee for Aeronautics,
Cleveland, Ohio.

APPENDIX A

SYMBOLS

The following symbols are used in this report:

A	cross-sectional area of blade, sq ft
B	parameter defined by equation (16)
C and C_I to C_{VI}	arbitrary constants
c_p	specific heat of gas at constant pressure, Btu/(lb)($^\circ$F)
D	length of orthogonal line, ft
Eu	Euler number, $\frac{x}{V_x}\frac{dV_x}{dx}$
Eu_{av}	integrated value of local Euler number, Eu
F	parameter defined by equation (16)
f	distance measured along orthogonal line, ft
G	parameter defined by equation (16)
g	acceleration due to gravity, ft/sec^2
H	average convective heat-transfer coefficient, Btu/(hr)(sq ft)($^\circ$F)
J	mechanical equivalent of heat, ft-lb/Btu
K	curvature or 1/r, 1/ft
k	thermal conductivity of blade unless otherwise indicated by subscripts, Btu/(hr)(ft)($^\circ$F)
k_B	constant value of thermal conductivity of blade, Btu/(hr)(ft)($^\circ$F)
L	total surface length, ft

l blade perimeter, ft

M Mach number, V/velocity of sound

m exponent for use in equation (1)

Nu average Nusselt number, $(Hl/\pi)/k_g$ (thermal conductivity evaluated at blade temperature)

Pr Prandtl number of gas, $3600\ gc_p\mu/k_g$ (properties evaluated at blade temperature)

p static pressure of gas, lb/sq ft

p' total pressure of gas, lb/sq ft

Q heat-flow rate, Btu/hr

R specific gas constant, ft-lb/(lb)(^oF)

Re average Reynolds number around blade, $(p_{av}V_{av}l/\pi)/RT_Bg\mu$ (properties evaluated at blade temperature)

Re_i inlet Reynolds number for blade, $(p_iV_il/\pi)/RT_Bg\mu$ (properties evaluated at blade temperature)

r radius of curvature, ft

Δr defined by $\Delta r = r_2 - r_1$, ft

s distance measured along flow lines, ft

T temperature, ^oR

T' total temperature of gas, ^oR

V velocity of gas, ft/sec

w weight flow, lb/sec

X parameter defined by $X^2 = V^2/2gJc_pT'$

x distance along surface from stagnation point, ft

Y value of y where $d\theta/dy = 0$, ft

y distance along blade axis measured from root, ft

α recovery factor

γ ratio of specific heats

η parameter defined by equation (16)

θ defined by $\theta = T_{g,e} - T_B$, $^{\circ}F$

θ_n value of θ at $y = 0$

λ constant

μ viscosity of gas, slugs/ft-sec

ξ transition ratio, ratio of length of laminar boundary layer on chordwise blade surface to total chordwise surface length

ρ static density, lb/cu ft

ρ' total density, lb/cu ft

φ defined by $\varphi^2 = \frac{lH}{k_B A}$

Subscripts:

1,2,3 surfaces or terms as indicated

av integrated average around blade

B at average blade temperature

c by convection

e effective value as applied to temperature

g gas

i inlet

n value of θ at $y = 0$

o outlet

x at local position x

y at local position y

$y+\Delta y$ at local position $y+\Delta y$

APPENDIX B

PROCEDURE FOR COMPUTING VELOCITY DISTRIBUTIONS

A sample flow channel is shown in figure 11 with f measured along the orthogonal line from surface 1 and s measured along the flow lines. The flow channel will be considered to be of unit depth.

For irrotational flow, the normal acceleration force on a differential mass at any point on the orthogonal line must be balanced by the pressure force along the orthogonal line, that is,

$$\frac{V^2\rho}{rg}\,ds\,df = \left(\frac{dp}{df}\,df\right)ds \tag{9}$$

By introducing Bernoulli's differential equation for compressible flow, equation (9) becomes

$$\frac{dV}{V} = -\,K\,df \tag{10}$$

In order to solve equation (10), K must be expressed as a known function of f. If the radius of curvature is expressed as a linear function of f, the curvature is given by

$$\frac{1}{K} = r_1 + \frac{r_2 - r_1}{D}\,f \tag{3}$$

From equation (3), df can be determined and substituted in equation (10), which can then be integrated. By integrating V between the limits V_1 and V, and K between the limits K_1 and K, the velocity can be expressed by the equation

$$\frac{V}{V_1} = \left(\frac{K}{K_1}\right)^{\frac{D}{\Delta r}} \tag{11}$$

where

$$\Delta r = r_2 - r_1$$

In order to determine the velocity from equation (11), V_1 must be known.

In order to evaluate V_1, the differential mass flow (per unit passage depth) for a compressible fluid is expressed by

$$dw = \rho' \left(1 - \frac{V^2}{2gJc_pT'}\right)^{\frac{1}{\gamma-1}} V \, df \tag{12}$$

For simplicity, let

$$X^2 = \frac{V^2}{2gJc_pT'} \tag{13}$$

By introducing equations (3) and (11) in equation (12) and integrating K between the limits K_1 and K_2 along the orthogonal line, the total mass flow through the channel becomes

$$\frac{w}{\rho'\sqrt{2gJc_pT'}} = -\int_{K_1}^{K_2} \left[1 - X_1^2 \left(\frac{K}{K_1}\right)^{\frac{2D}{\Delta r}}\right]^{\frac{1}{\gamma-1}} X_1 \left(\frac{K}{K_1}\right)^{\frac{D}{\Delta r}} \frac{D}{\Delta r K^2} \, dK \tag{14}$$

Because equation (14) cannot be directly integrated, it is convenient to rewrite the bracketed term as

$$\left[1 - X_1^2 \left(\frac{K}{K_1}\right)^{\frac{2D}{\Delta r}}\right]^{\frac{1}{\gamma-1}} = \left(1 - X_1^2\right)^{\frac{1}{\gamma-1}} \left\{1 - \frac{X_1^2}{1 - X_1^2} \left[\left(\frac{K}{K_1}\right)^{\frac{2D}{\Delta r}} - 1\right]\right\}^{\frac{1}{\gamma-1}} \tag{15}$$

Because

$$\frac{X_1^2}{1 - X_1^2} \left[\left(\frac{K}{K_1}\right)^{\frac{2D}{\Delta r}} - 1\right]$$

is small compared with 1, the left expression of equation (15) can be expanded by the binomial theorem and all terms except the first two may be neglected. Equation (14) can then be integrated. When integrated and simplied with

$$\left.\begin{aligned} B &= D/\Delta r \\ F &= \frac{B}{B-1}\left[\left(\frac{K_2}{K_1}\right)^{B-1} - 1\right] \\ G &= \frac{B}{3B-1}\left[\left(\frac{K_2}{K_1}\right)^{3B-1} - 1\right] \\ \eta &= \frac{-wK_1}{G\rho'\sqrt{2gJc_pT'}} \end{aligned}\right\} \tag{16}$$

the total mass flow is given by

$$\eta = X_1^3 \frac{(1 - X_1^2)^{\frac{2-\gamma}{\gamma-1}}}{\gamma - 1}\left[\left(\frac{(\gamma-1)(1-X_1^2)}{X_1^2} + 1\right)\frac{F}{G} - 1\right] \tag{17}$$

For a particular flow channel with given flow conditions, the only unknown in equation (17) is X_1. Therefore, if the flow network (flow lines and orthogonal lines) is constructed, the value of X at surface 1 can be determined for any orthogonal line. From equation (13) the corresponding velocity is computed. The velocity on the same orthogonal line but at surface 2 is then computed by equation (11).

Because equation (17) presents a trial-and-error solution for X_1, it is more convenient to determine X_1 graphically. For this reason, equation (17) has been plotted for different values of γ and F/G in figure 12.

APPENDIX C

DEVELOPMENT OF HEAT-TRANSFER-COEFFICIENT EQUATIONS

For a turbine blade of constant cross-sectional area heated or cooled at the root and subjected to a cross flow of air, a simple heat balance can be made across any increment of length Δy along the y-axis of the blade (y is measured from the root). This heat balance (which expresses the heat flow at y minus the heat flow at $y+\Delta y$ equal to the heat added to Δy by convection) is given by

$$Q_y - Q_{y+\Delta y} = Q_c \tag{18}$$

If Δy is made small, the heat flow at y and that at $y+\Delta y$ are related by

$$Q_{y+\Delta y} = Q_y - \frac{dQ}{dy}\,dy$$

The convective heat flow is

$$Q_c = Hl\,dy\,(T_{g,e} - T_{B,y})$$

Therefore for $Q_y = -kA\,\frac{dT_{B,y}}{dy}$, equation (18) becomes

$$A\,\frac{dT_{B,y}}{dy}\,\frac{dk}{dy} + Ak\,\frac{d^2T_{B,y}}{dy^2} = -Hl(T_{g,e} - T_{B,y}) \tag{19}$$

With the conductivity defined by

$$k = k_B\left[1 - \lambda(T_{g,e} - T_{B,y})\right]$$

(which expresses the conductivity as a linear function of the blade temperature, because the gas temperature remains constant for any particular case) and the temperature difference defined by

$$\theta = T_{g,e} - T_{B,y}$$

equation (19) reduces to

$$(1 - \lambda\theta)\frac{d^2\theta}{dy^2} - \lambda\left(\frac{d\theta}{dy}\right)^2 - \frac{lH}{Ak_B}\theta = 0 \tag{20}$$

A solution of equation (20) will give the one-dimensional temperature distribution in the turbine blade. A solution can be made by assuming $\lambda = 0$ (constant k) or $\lambda \neq 0$ (variable k). These two cases will be considered.

Constant Thermal Conductivity

If λ is set equal to zero and k_B is taken at the average blade temperature, equation (20) reduces to

$$\frac{d^2\theta}{dy^2} - \varphi^2\theta = 0 \tag{21}$$

where

$$\varphi^2 = \frac{lH}{Ak_B}$$

A well-known solution to this equation is

$$\theta = C_I \cosh \varphi(C_{II} - y) \tag{22}$$

The boundary conditions applicable for the experimental investigations are

$$\begin{aligned} \frac{d\theta}{dy} &= 0 \quad \text{at} \quad y = Y \\ \theta &= \theta_n \quad \text{at} \quad y = 0 \end{aligned} \tag{23}$$

and equation (22) becomes

$$\theta = \theta_n \frac{\cosh \varphi(Y - y)}{\cosh \varphi Y} \tag{4}$$

Variable Thermal Conductivity

If λ is not equal to zero, a solution of equation (20) can be written in the form

$$\theta = \theta_1 + \lambda\theta_2 + \lambda^2 \theta_3 + \ldots \tag{24}$$

where θ_1 is the solution for $\lambda = 0$ ($k = k_B$), and $\lambda\theta_2 + \lambda^2 \theta_3 + \ldots$ are corrections for a variable thermal conductivity. Therefore with

$$\varphi^2 = \frac{lH}{k_B A}$$

and

$$k = k_B(1 - \lambda\theta)$$

θ_1 (similar to θ in equation (22)) becomes

$$\theta_1 = C_{III} \cosh \varphi(C_{IV} - y) \tag{25}$$

When equation (25) is substituted in equation (24), θ is

$$\theta = C_{III} \cosh \varphi(C_{IV} - y) + \lambda\theta_2 + \lambda^2 \theta_3 \ldots \tag{26}$$

Taking the necessary derivatives of equation (26) and neglecting powers of λ higher than 1 (using only a first-order correction because λ is small), changes equation (20) to

$$\frac{d^2\theta_2}{dy^2} - \varphi^2 \theta_2 = C_{III}^2 \varphi^2 \cosh 2\varphi(C_{IV} - y) \tag{27}$$

Equation (27) has a solution of the form

$$\theta_2 = C_V \cosh \varphi(C_{VI} - y) + \frac{C_{III}^2}{3} \cosh 2\varphi(C_{IV} - y) \tag{28}$$

From equations (25) and (28), the solution of equation (20) is therefore

$$\theta = C_{III} \cosh \varphi(C_{IV} - y) + \lambda\left[C_V \cosh \varphi(C_{VI} - y) + \frac{C_{III}^2}{3} \cosh 2\varphi(C_{IV} - y)\right] \tag{29}$$

For the boundary conditions stated by equation (23) and matching θ_1 and θ at $y = 0$, the constants in equation (29) can be determined and final solution of equation (20) becomes

$$\theta = \left(\frac{\theta_n}{\cosh \varphi Y} - \frac{\lambda\theta_n^2 \cosh 2\varphi Y}{3 \cosh^3 \varphi Y}\right) \cosh \varphi(Y - y) + \lambda\theta_n^2 \frac{\cosh 2\varphi(Y - y)}{3 \cosh^2 \varphi Y} \tag{5}$$

REFERENCES

1. Pollmann, Erich: Temperatures and Stresses on Hollow Blades for Gas Turbines. NACA TM 1183, 1947.

2. Andrews, S. J., and Bradley, P. C.: Heat Transfer to Turbine Blades. Memo. No. M.37, Nat. Gas Turbine Establishment, M.A.P. (London), Oct. 1948.

3. Bammert, K., and Hahneman, H.: Heat Transfer in the Gas Surrounding Cooled Gas Turbine Blades. Part 3: Results of the Experiments. Reps. & Trans. No. 620, GDC 2466, British M.O.S., Aug. 29, 1946.

4. Meyer, Gene L.: Determination of Average Heat-Transfer Coefficients for a Cascade of Symmetrical Impulse Turbine Blades. I - Heat Transfer from Blades to Cold Air. NACA RM E8H12, 1948.

5. Hubbartt, James E.: Comparison of Outside-Surface Heat-Transfer Coefficients for Cascades of Turbine Blades. NACA RM E50C28, 1950.

6. Freche, John C., and Schum, Eugene F.: Determination of Gas-to-Blade Convection Heat-Transfer Coefficients on a Forced-Convection, Water-Cooled, Single-Stage Aluminum Turbine. NACA RM E50J23, 1950.

7. Brown, W. Byron, and Donoughe, Patrick L.: Extension of Boundary-Layer Heat-Transfer Theory to Cooled Turbine Blades. NACA RM E50F02, 1950.

8. Huppert, M. C., and MacGregor, Charles: Comparison between Predicted and Observed Performance of Gas-Turbine Stator Blade Designed for Free-Vortex Flow. NACA TN 1810, 1949.

9. Livingood, John N. B., and Brown, W. Byron: Analysis of Spanwise Temperature Distribution in Three Types of Air-Cooled Turbine Blade. NACA Rep. 994, 1950.

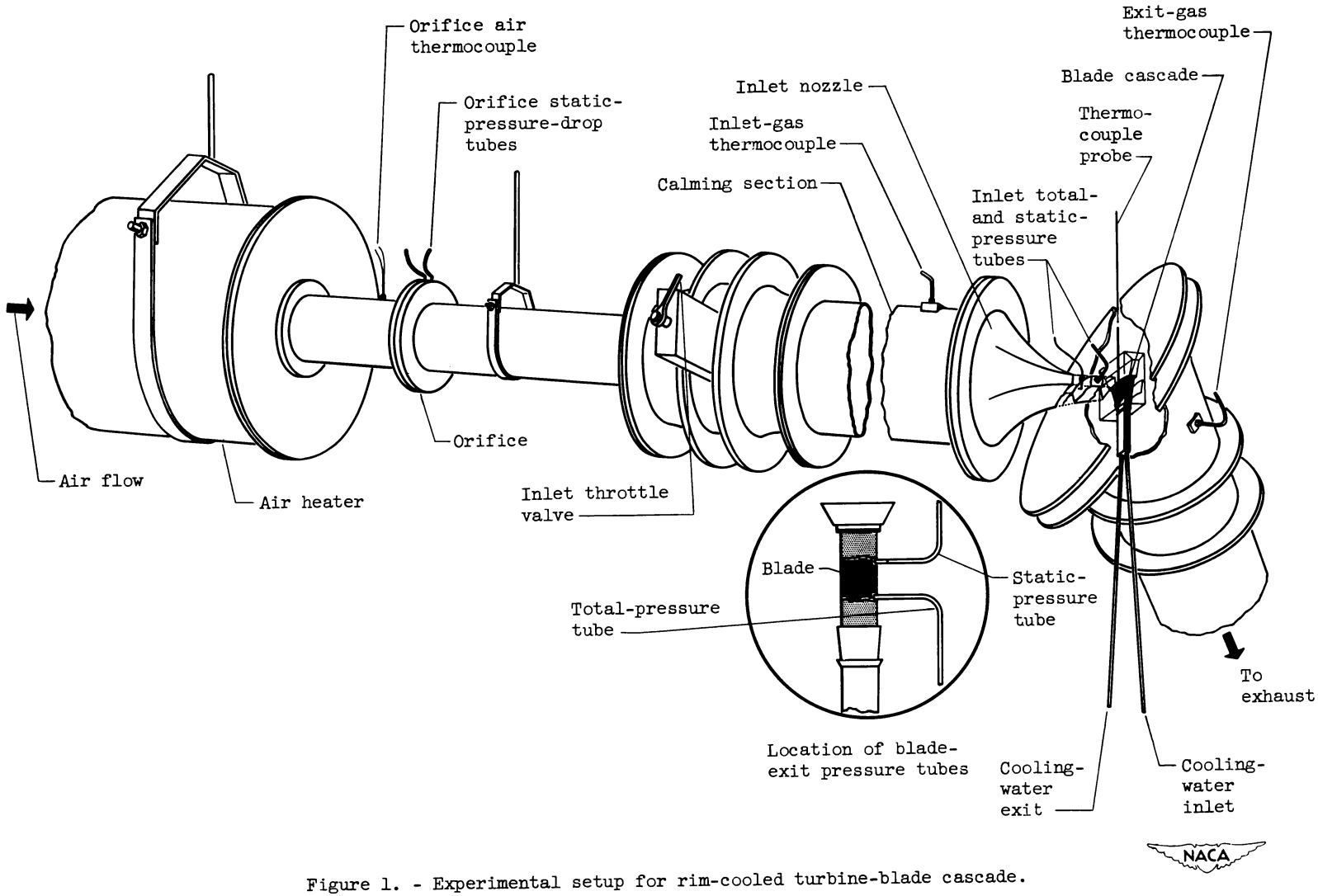

Figure 1. - Experimental setup for rim-cooled turbine-blade cascade.

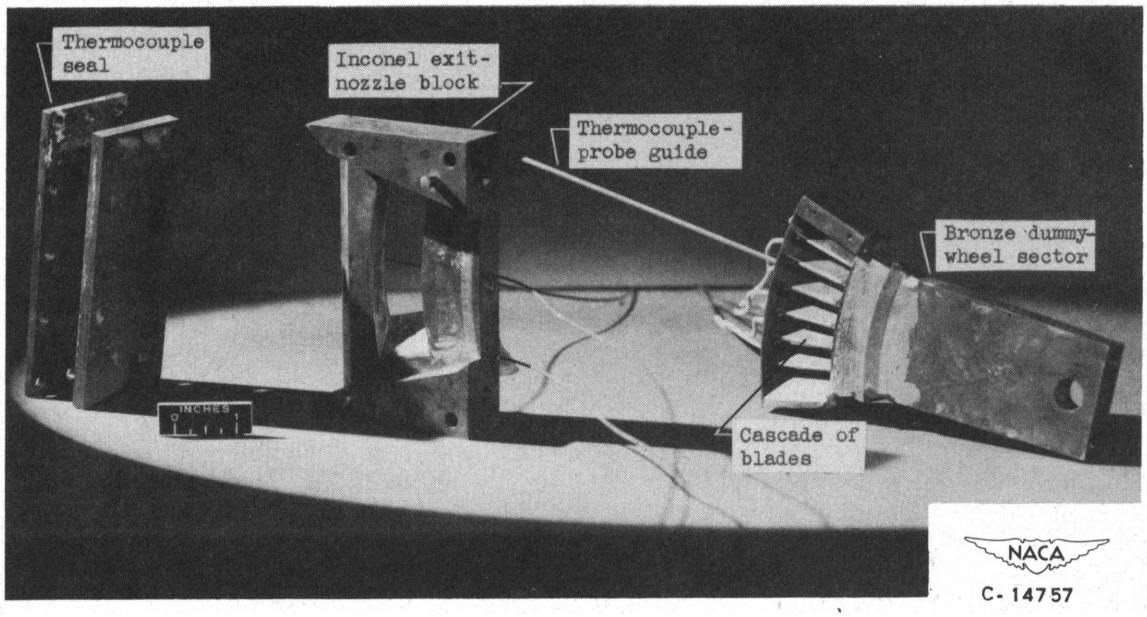

(a) Unassembled.

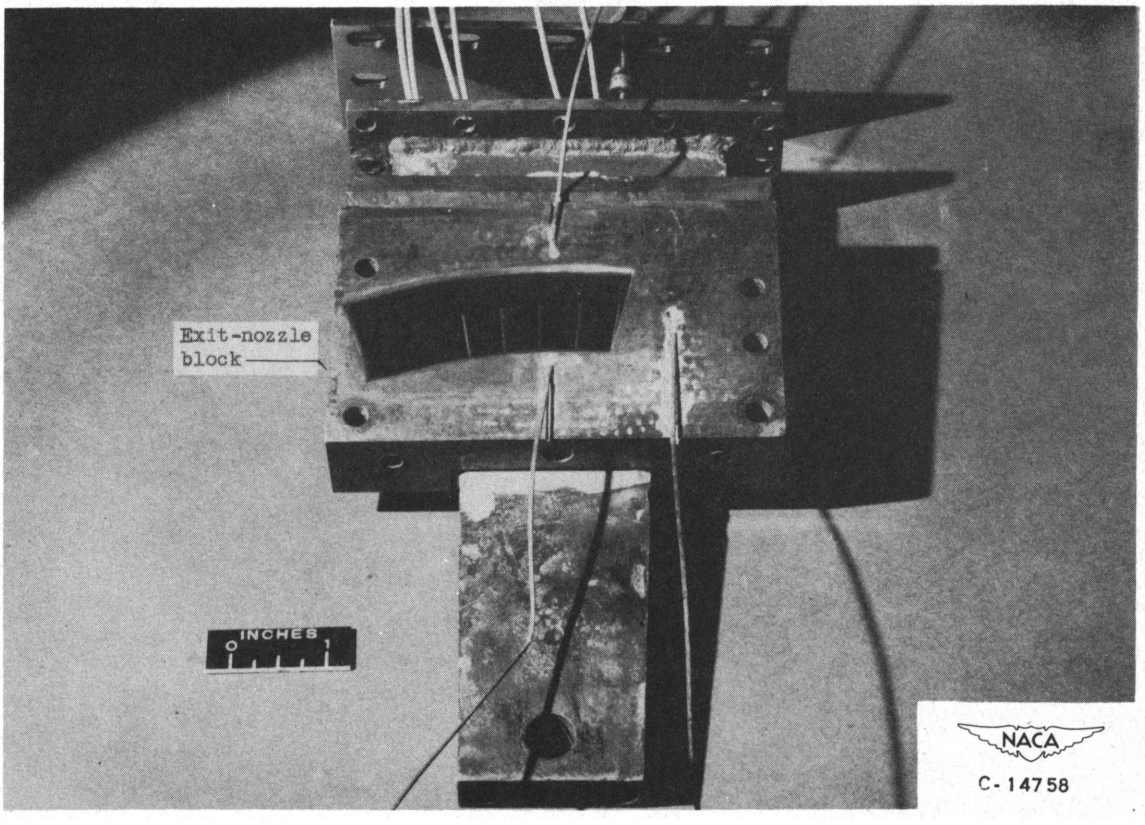

(b) Assembled.

Figure 2. - Special experimental rig for heat-transfer studies of symmetrical impulse turbine blades.

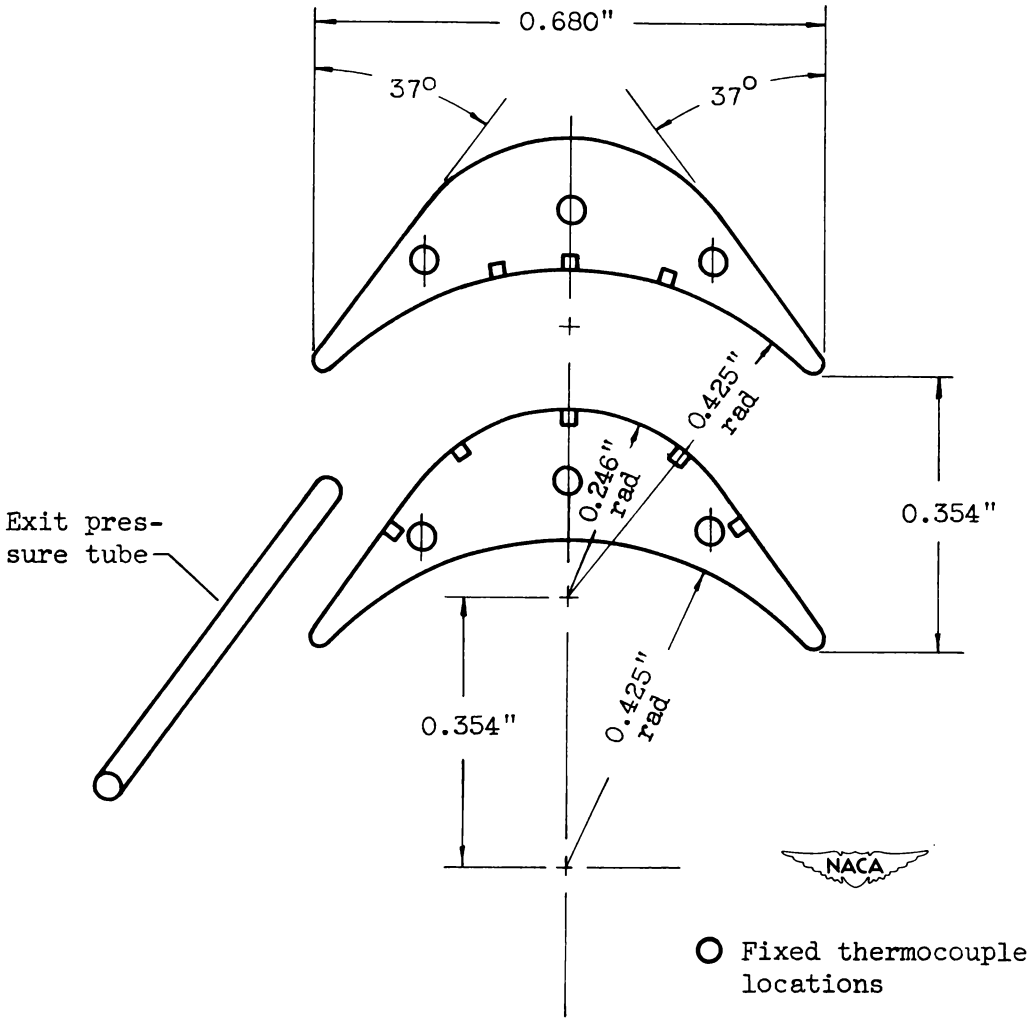

Chord, in.	0.680
Perimeter, in.	1.785
Constant cross-sectional area, sq in.	0.0797
Pitch-line radius, in.	5.50
Number of blades in 360°	84
Chord-to-pitch ratio	1.92

Figure 3. - Cross sections of symmetrical impulse turbine blades.

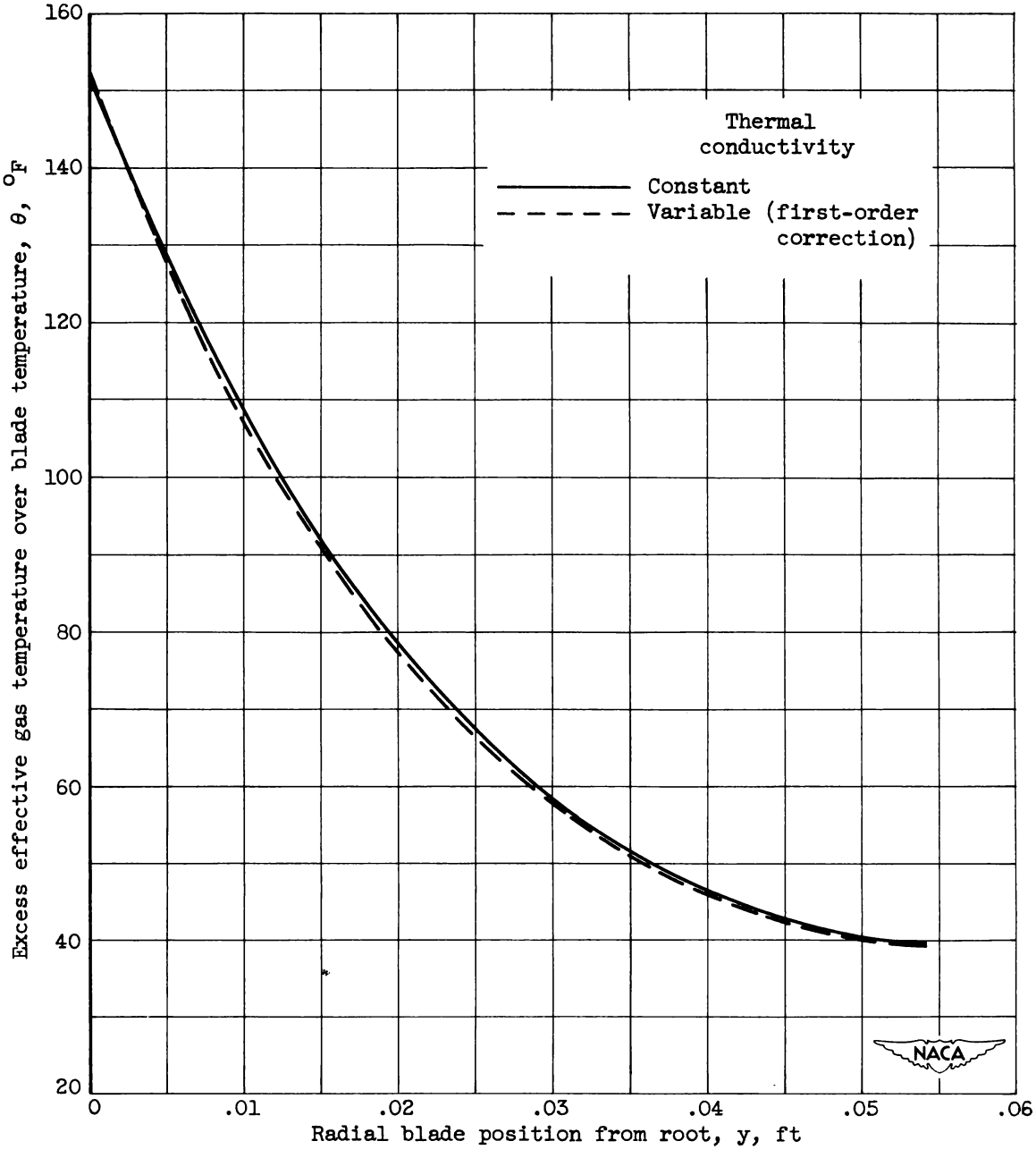

Figure 4. - Comparison of theoretical temperature distributions for constant and variable thermal conductivity.

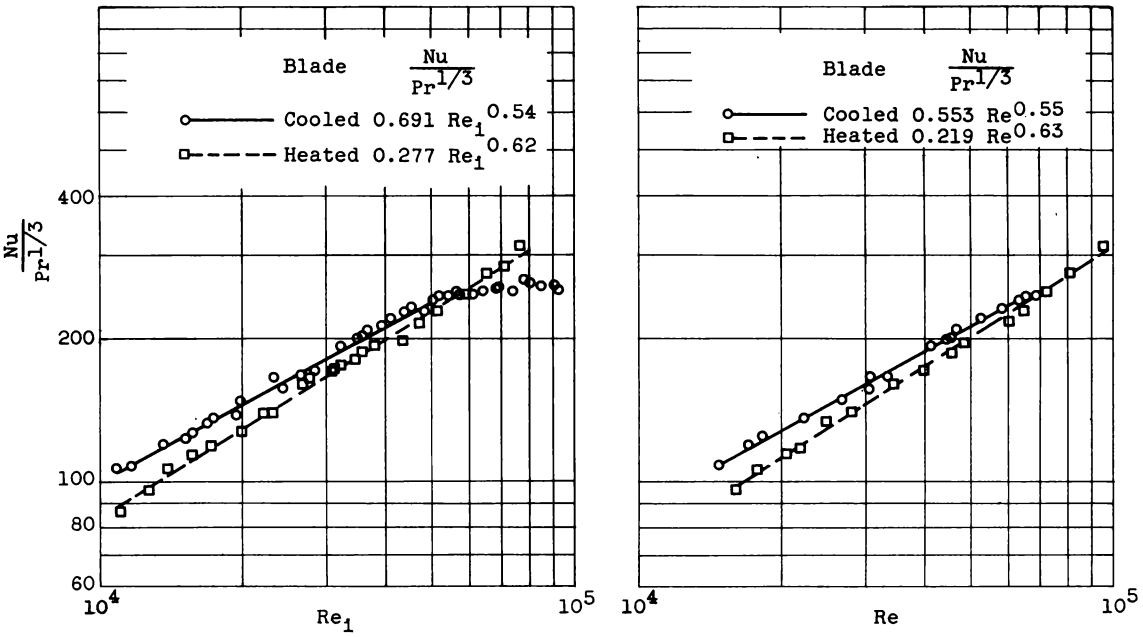

(a) Reynolds number evaluated with inlet velocity and pressure.

(b) Reynolds number evaluated with average velocity and average pressure around blade periphery.

Figure 5. - Comparison of heat-transfer results from heated and cooled blades. Gas properties and density based on average blade temperature.

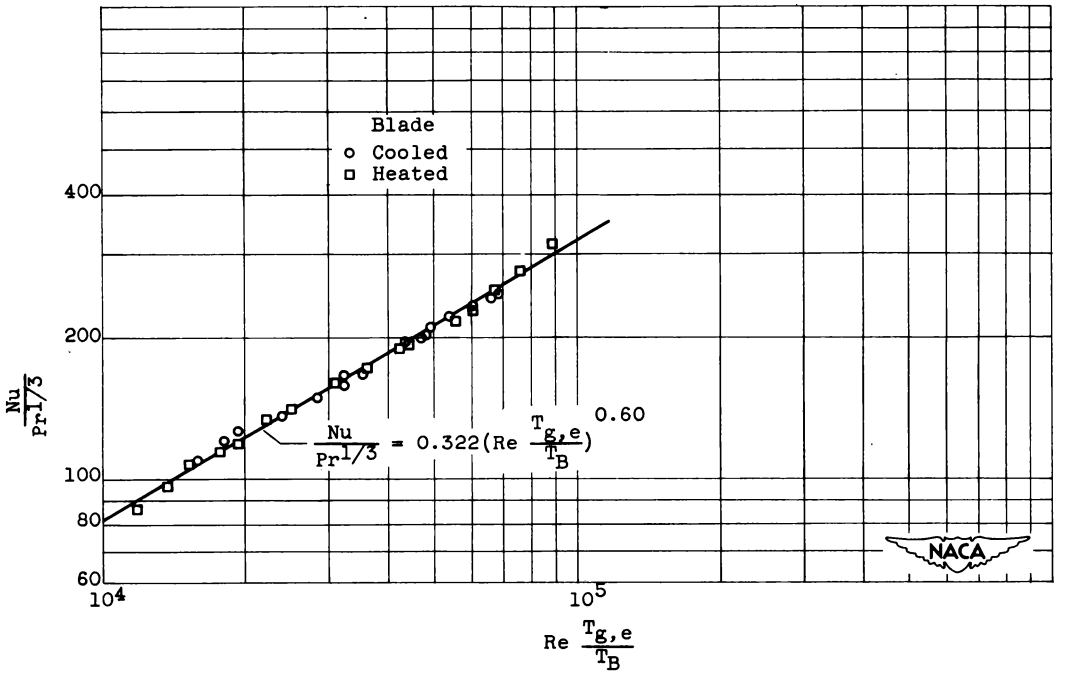

Figure 6. - Correlation of heat-transfer results from both heated and cooled blades. Gas properties and density based on average blade temperature; Reynolds number evaluated with average velocity and average pressure around blade periphery.

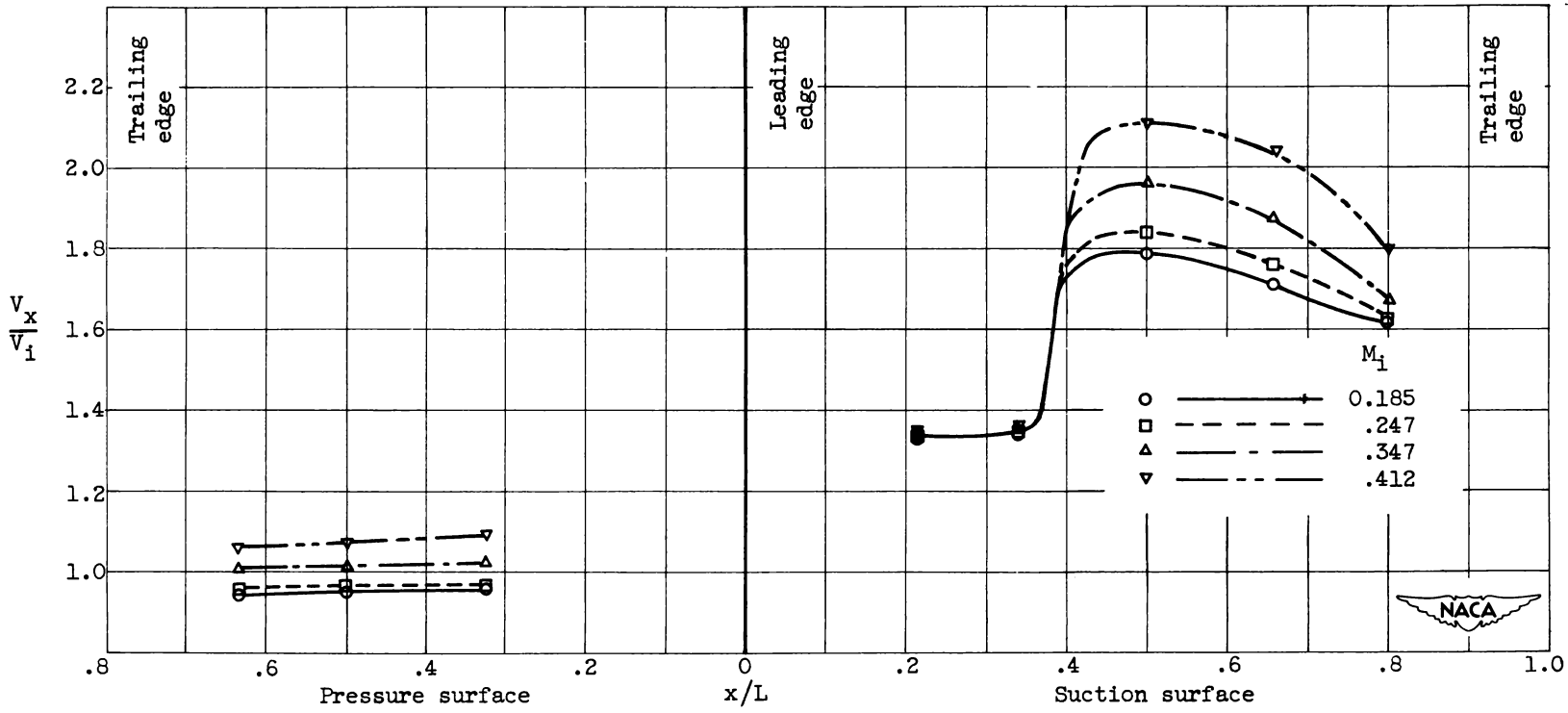

Figure 7. - Experimental velocity distributions for an impulse-type blade and effect of Mach number upon experimental velocity distribution.

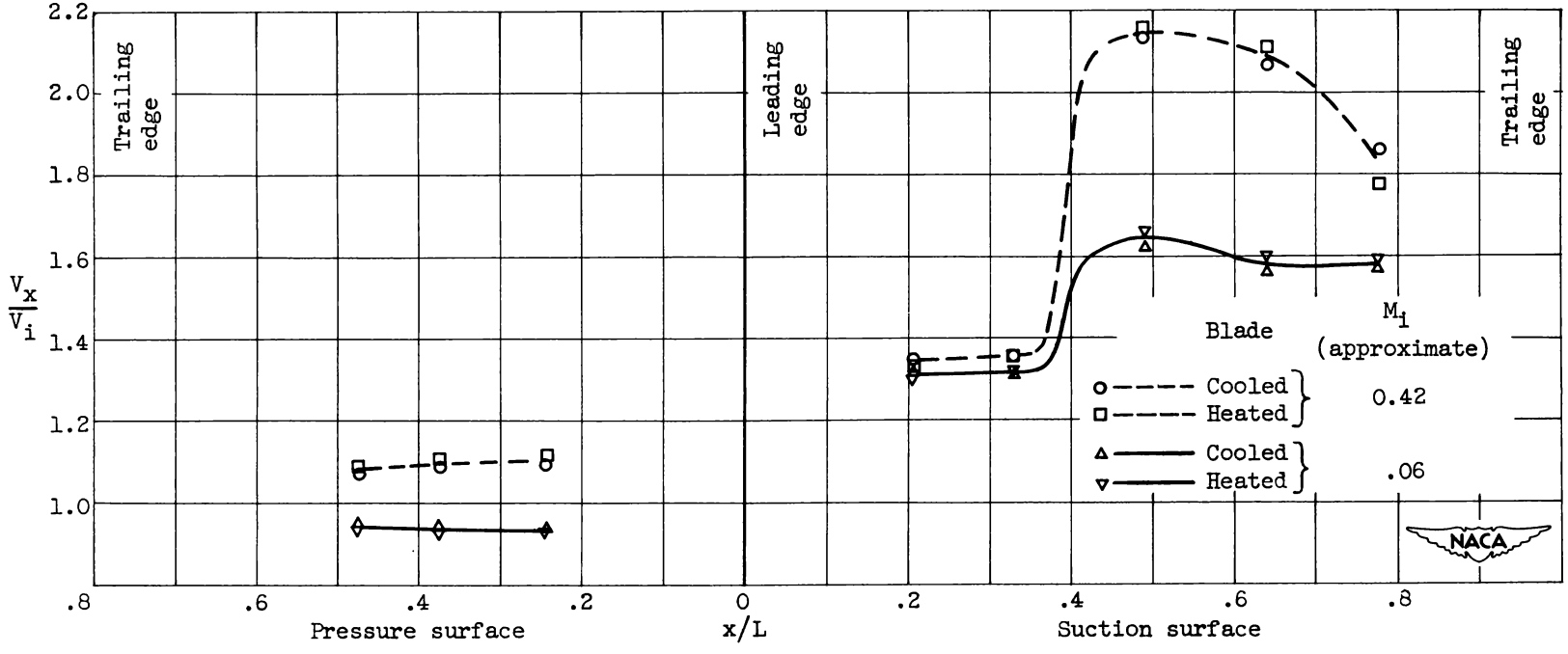

Figure 8. - Comparison of experimental velocity distributions for cooled and heated impulse-type blade.

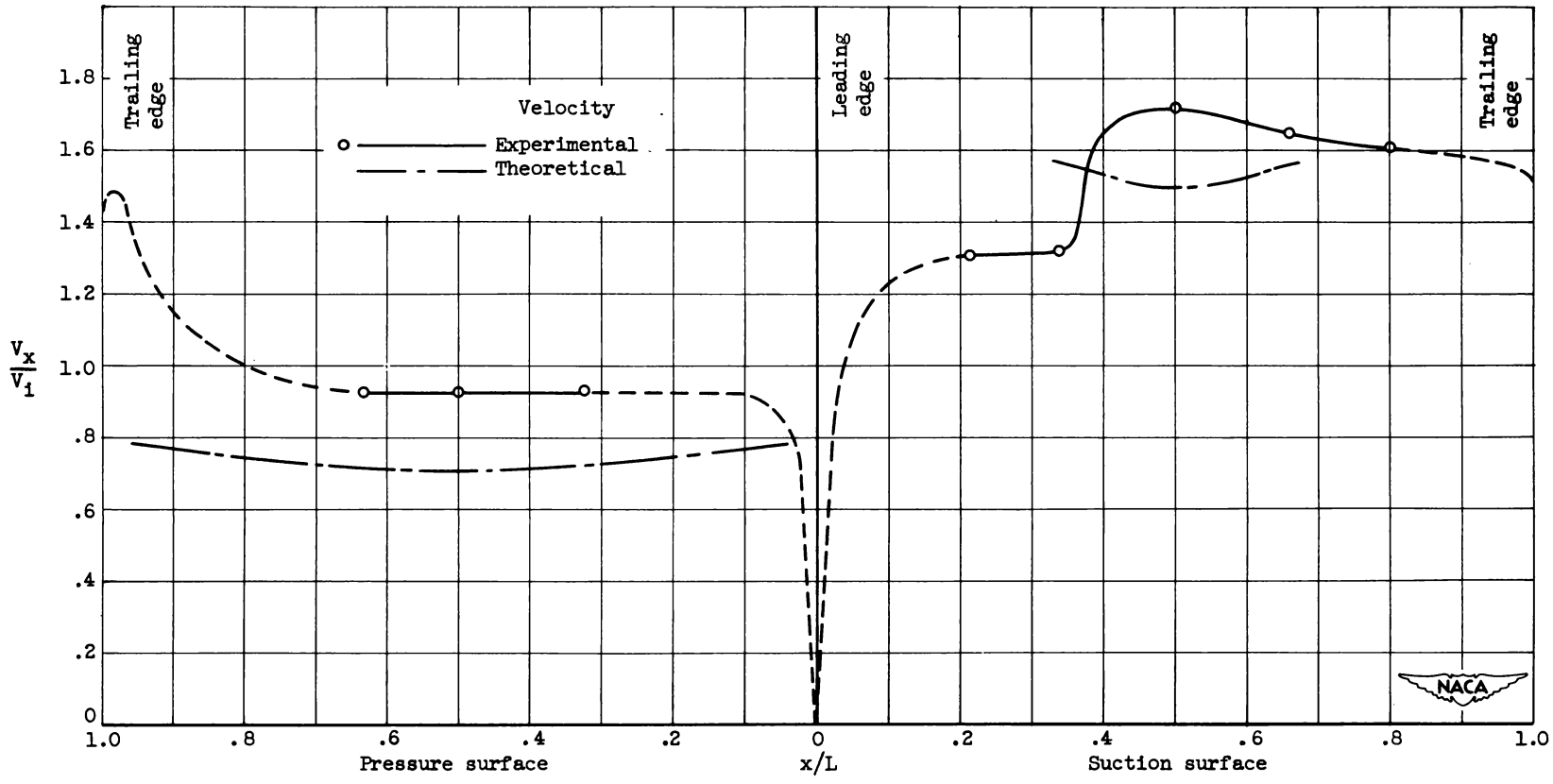

Figure 9. - Comparison of experimental and theoretical velocity distributions for impulse-type blade. Inlet Mach number, approximately 0.12.

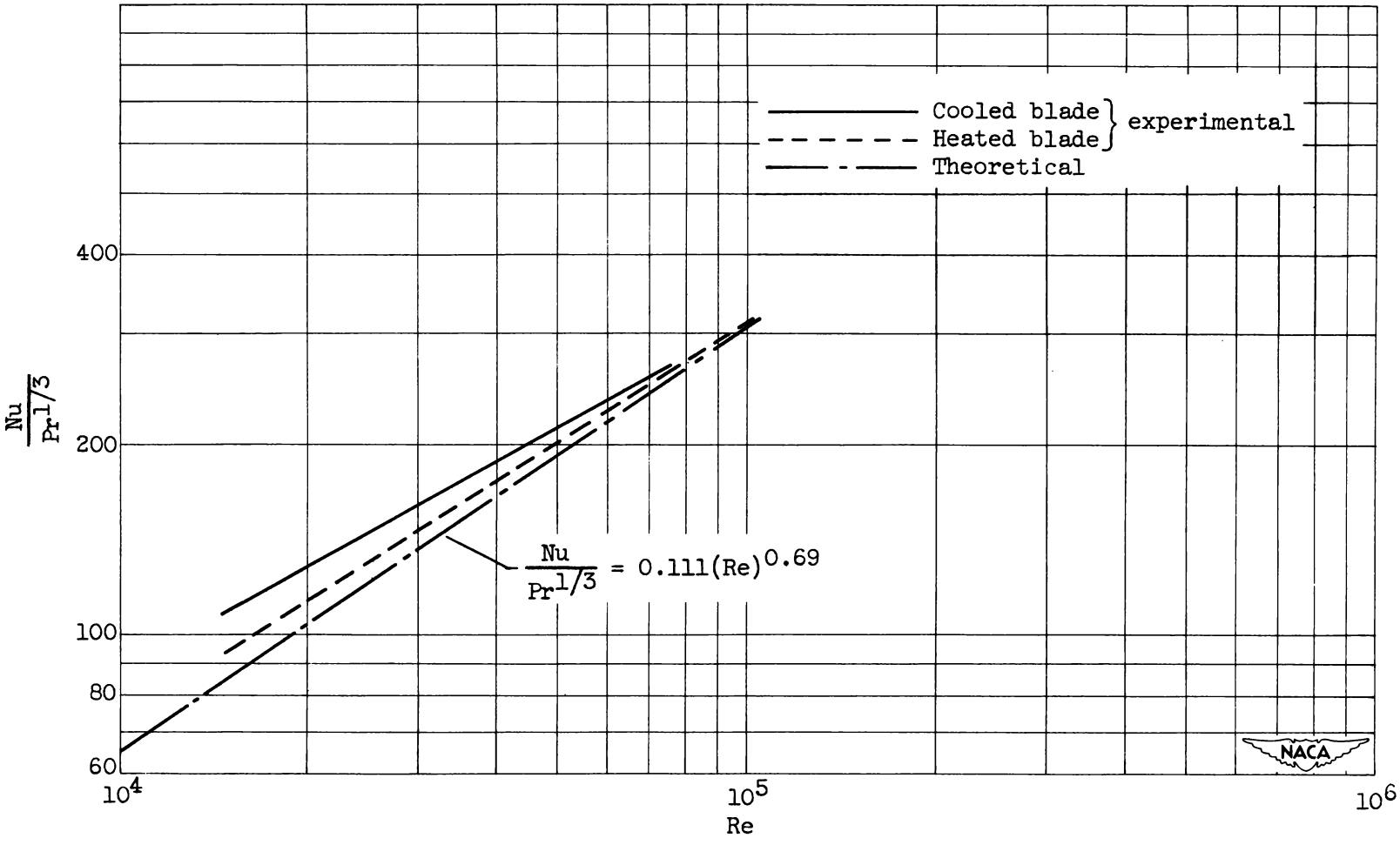

Figure 10. - Comparison of experimental and theoretical heat-transfer correlations. Gas properties and density based on average blade temperature; Reynolds number evaluated with average velocity and average pressure around blade periphery.

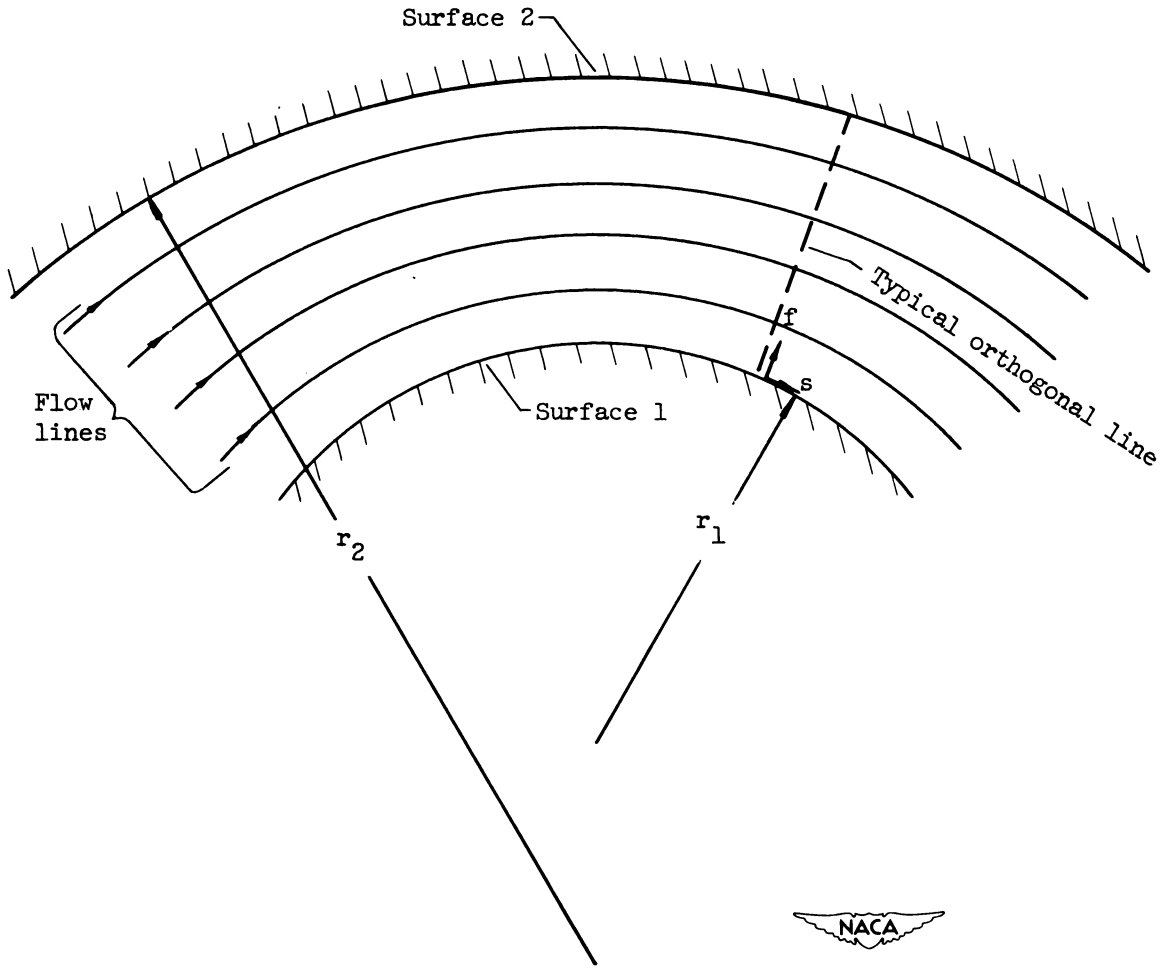

Figure 11. - Sample flow channel.

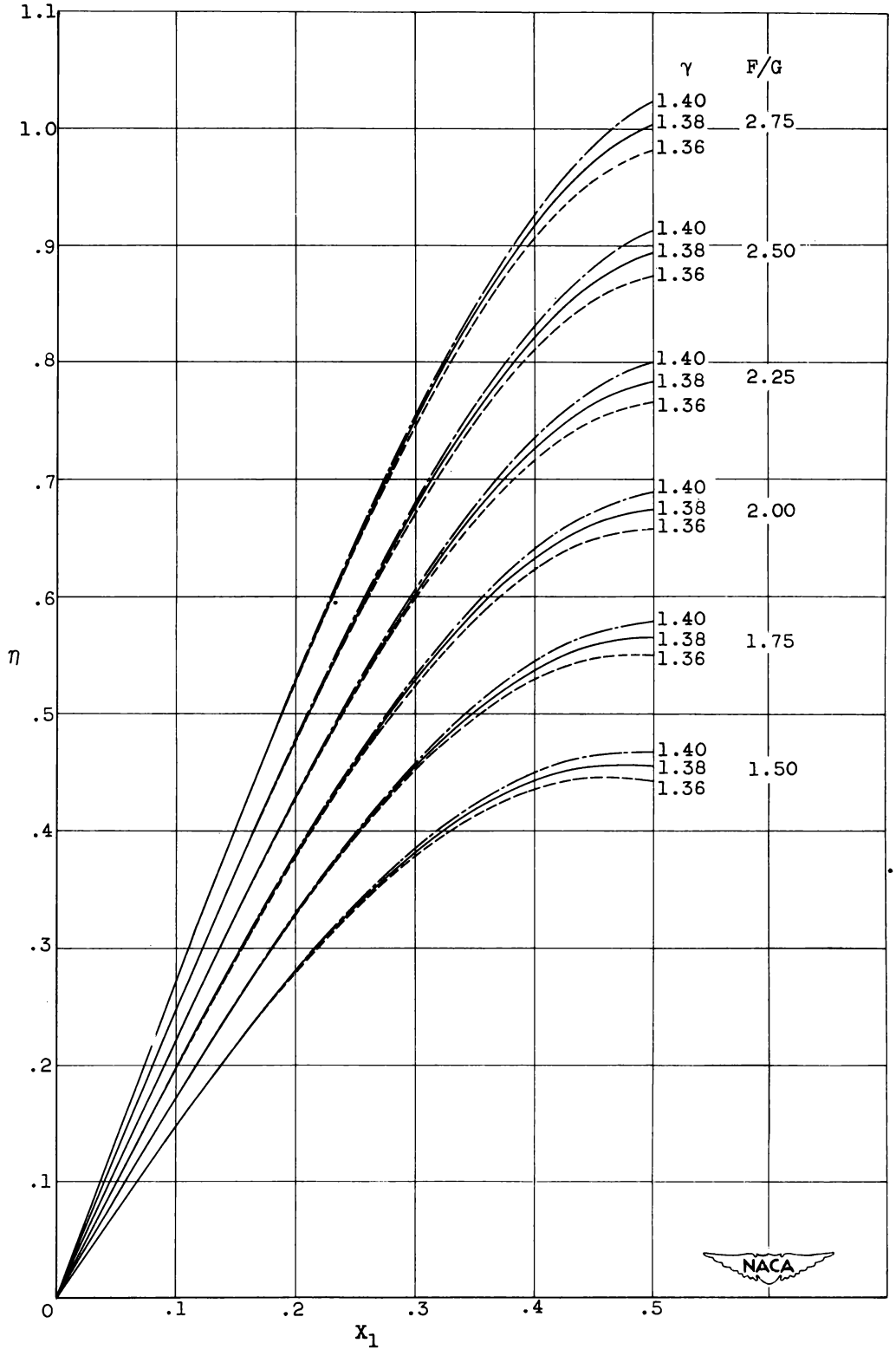

Figure 12. - Variation of η with X_1 for values of γ and F/G. (A 10- by 18-in. print of this fig. is attached.)

NACA-Langley - 3-9-51 - 475

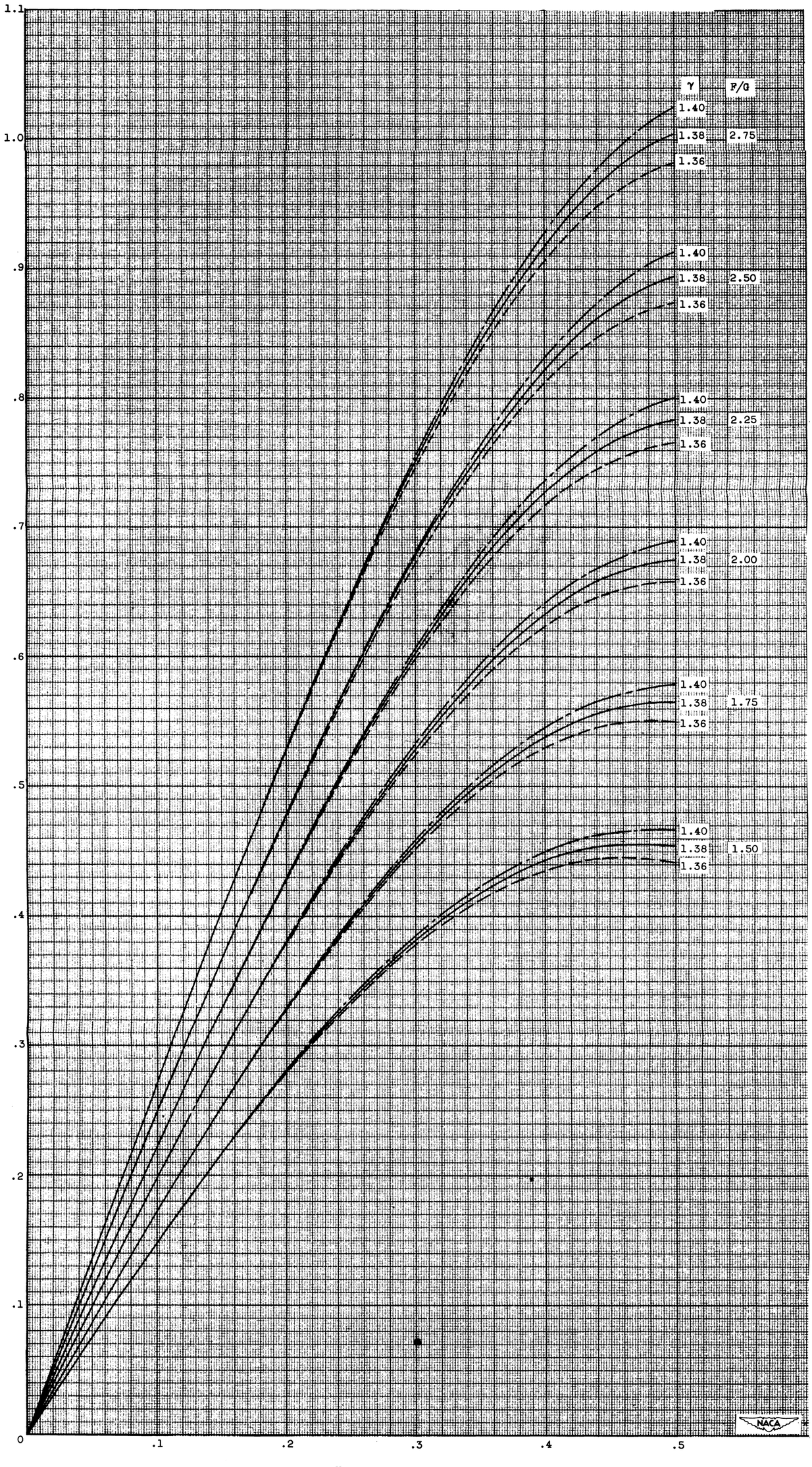

Figure 12. - Variation of η with X_1 for values of γ and F/G.